

Using a Node Positioning Algorithm to Improve Models of Groundwater Flow Based on Meshless Methods

BRYCE D. WILKINS¹, THEODORE V. HROMADKA II², WILLIAM NEVILS³, BENJAMIN SIEGEL³, PRARABDHA YONZON³

¹ Carnegie Mellon University, United States of America

² Distinguished Professor, United States Military Academy, United States of America

³ Cadet, United States Military Academy, United States of America

ABSTRACT

Recently, the Computational Engineering Mathematics program at the United States Military Academy has made significant advancements in determining suitable locations of nodal points (or model sources) for use in meshless numerical methods for partial differential equations such as the Complex Variable Boundary Element Method (CVBEM). The latest node positioning algorithm (NPA) to emerge from the group was used to develop high-precision outcomes for several benchmark problems in potential flow. Such high-precision outcomes provide more confidence in the predictions obtained for various geoscience results. For example, groundwater flow models are of high importance to many areas of analysis in which a key point of investigation is determination of the location of a source of contamination given a location of damage downstream caused by accumulation of the contamination. The improved computational accuracy afforded by the coupled CVBEM/NPA models buttresses the other forms of evidence typically used in performing such a forensics analysis including geochemical testing and dating of chemical compounds, among other techniques. In this paper, we apply the recent NPA to model a new set of challenging computational problems with the goal of identifying the likely source of a hypothetical contamination among a set of candidate sources.

Keywords: *contamination detection, potential flow, Complex Variable Boundary Element Method (CVBEM), node positioning algorithms (NPAs), mesh reduction methods, applied complex variables*

1 INTRODUCTION

The Complex Variable Boundary Element Method (CVBEM) [1, 2] is a numerical procedure for approximating the solution of boundary value problems (BVPs) of the Laplace and related partial differential equations (PDEs) [3, 4]. In the early 2000's, the CVBEM methodology was extended to modeling BVPs in three and higher spatial dimensions [5, 6]. Recent developments have focused on developing algorithms for determining suitable locations of collocation points and computational nodes for use in CVBEM models [7, 8, 9]. The CVBEM is related to other mesh reduction numerical methods for PDEs including the real variable boundary element methods [10, 11] and the Method of Fundamental Solutions (MFS) [12, 13]. Several studies have focused on the application of the CVBEM to groundwater

modeling and contaminant transport, and this work builds upon these studies [14, 15, 16].

The CVBEM approximation function is constructed as a linear combination of complex variable basis functions that are each analytic within a prescribed simply-connected problem domain, Ω :

$$\hat{\omega}(z) = \sum_{j=1}^n c_j g_j(z), \quad z \in \Omega, \quad (1)$$

where $c_j \in \mathbb{C}$ denotes a complex coefficient and $g_j : \mathbb{C} \rightarrow \mathbb{C}$ is analytic within Ω . Since c_j is a complex coefficient, it has two parts: a real part and an imaginary part. Thus, for n coefficients, there are $2n$ unknown values that need to be determined in the CVBEM modeling process. These coefficients can be determined in a number of ways including by collocation or least squares minimization. When collocation is used, it is necessary to specify $2n$ collocation points on the problem boundary where the value of the boundary conditions are known and will be enforced. In this case, the coefficients of Equation (1) are determined so that the CVBEM approximation function matches the specified boundary conditions at the given collocation points with the exception of possible truncation, round-off, and other numerically-introduced errors.

Importantly, since the basis functions are selected such that they are analytic within Ω , the CVBEM approximation function is a linear combination of analytic functions and is, therefore, analytic itself. Therefore, the real and imaginary parts of the CVBEM approximation function are related by the Cauchy-Riemann equations:

$$\frac{\partial \hat{\phi}}{\partial x} = \frac{\partial \hat{\psi}}{\partial y} \quad \text{and} \quad \frac{\partial \hat{\phi}}{\partial y} = -\frac{\partial \hat{\psi}}{\partial x}. \quad (2)$$

From the Cauchy-Riemann equations, it follows that the real and imaginary parts of the CVBEM approximation function are harmonic functions. That is,

$$\begin{aligned} \Delta \hat{\phi} &= 0 \quad \text{where } \hat{\phi}(x, y) = \Re[\hat{\omega}(z)], \quad (x + iy) \in \Omega \\ \Delta \hat{\psi} &= 0 \quad \text{where } \hat{\psi}(x, y) = \Im[\hat{\omega}(z)], \quad (x + iy) \in \Omega. \end{aligned} \quad (3)$$

Consequently, since the real and imaginary parts of the CVBEM approximation function satisfy Laplace's equation, the error of the approximation function is assessed by examining the closeness of fit of the approximation function to the specified boundary conditions. The maximum error of the CVBEM approximation function can be assessed using the maximum modulus principle for harmonic functions [17]. This is done by determining the maximum departure on the problem boundary of the CVBEM approximation function from the specified boundary conditions. That is, the maximum error, E , can be expressed as:

$$E = \max_{(x,y) \in \partial\Omega} |\hat{\phi}(x, y) - \phi(x, y)|, \quad (4)$$

where $\phi(x, y)$ denotes the target potential function.

Additionally, since $\hat{\phi}$ and $\hat{\psi}$ are conjugate functions, their level curves are orthogonal, resulting in the well-known flownet graphical display that applies to numerous applications in science, mathematics, engineering, and related fields [18]. This dual harmonic function outcome in the CVBEM is of particular value when analyzing boundary value problems of the mixed type. Such properties do not similarly exist for real valued functions and associated computational methods such as the finite difference method or finite element method (FEM). This is a principal motivation for using CVBEM-type approximation functions to solve problems that occur in the many fields involved with the geosciences as well as other technical areas.

In this work, the coupled CVBEM/NPA approach is used to computationally solve difficult problems of groundwater flow where high-precision modeling outcomes are needed. The focus is to provide further evidence to supplement the usual geochemical evidence in order to determine the source of a contaminant in the groundwater from among a set of candidate source points given the location of the downstream contamination site [19].

2 SUMMARY OF NPA PROCEDURES AND APPLYING AN NPA TO THE CVBEM

An important step in the modeling procedure is the selection of computational nodes, which are the branch points of the basis functions. Originally, the CVBEM methodology called for placing nodes on the problem boundary [2]. More recent implementations of the CVBEM have relaxed this constraint and used computational nodes located in the exterior of $\Omega \cup \partial\Omega$, which is similar to the approach taken in the MFS [20]. The next evolution of the procedure has involved the development and utilization of NPAs to systematically locate computational nodes with the goal of reducing computational model error [8, 9].

In general, the NPAs under study by our research group have the following steps:

1. Generate an initial distribution of candidate computational nodes and candidate collocation points. The candidate collocation points are located on the problem boundary and are where the boundary conditions are enforced. The candidate computational nodes are located in the exterior of $\Omega \cup \partial\Omega$.
2. Initialize the NPA by selecting two collocation points to be used in the CVBEM model. Two collocation points are needed for the reason described above, which is that each complex coefficient of Equation (1) has two real parts. These unknown real values are determined by collocation. Therefore, each node corresponds to two collocation points.
3. For each of the candidate computational nodes, create a new CVBEM model by adding the candidate node to the current CVBEM model. Evaluate each of these models to determine the maximum error on the problem boundary using Equation (4) that corresponds to the use of the particular candidate node. Recall, the maximum error of the CVBEM approximation function is known to occur on the problem boundary as a consequence of

the maximum modulus principle. After evaluating each of these models, select the model that resulted in the least error in satisfying the given boundary conditions, and add the appropriate node to the CVBEM model.

4. Evaluate the error on the boundary of the CVBEM approximation function using Equation (4). Select two new collocation points to be located on the problem boundary at the two greatest local maxima of the error function.
5. Repeat Steps 3 and 4 until $2n$ collocation points have been selected and n computational nodes have been selected. The final CVBEM model will consist of these $2n$ collocation points and n computational nodes. This model can be used to generate flownet graphical displays of the potential problem.

Variations of the procedure discussed in these steps have been considered. For example, the NPA discussed in [9] incorporates a refinement procedure, which is used to re-evaluate the utility of previously-selected computational nodes and potentially replace those nodes with different nodes if it is found that the replacement further reduces the error of the CVBEM model.

However, the common feature of the recent NPAs used by our group is that the algorithm proceeds by alternately selecting two collocation points followed by one computational node. This is important because the challenge of selecting each node is reduced to a single variable optimization problem since the only quantity that is varying is the location of the computational node to be added to the CVBEM model. Ordinarily, such optimization problems are solved by taking the partial derivative of an objective function and setting the result equal to zero. In this case, the objective function is Equation (4), and we solve this problem computationally by exhaustively testing each candidate computational node to determine which one optimizes the objective function by resulting in the CVBEM model of least error.

While it can be computationally expensive to use these NPAs, the benefit of using them is that it is possible to achieve highly efficient uses of computational nodes and collocation points. That is, using these NPAs can result in CVBEM models that use relatively few nodes and collocation points, but still achieve the same or better accuracy compared to much larger CVBEM models where the locations of the collocation points and nodes have not been determined by an NPA.

3 PROBLEM DESCRIPTION

In this work, we consider three different example problems in which the goal is to determine the source of accumulated groundwater contamination detected downstream from a set of candidate source points. In these example problems, we have hypothesized that one of the candidate source points is a Leaking Underground Storage Tank (LUST), which is the true source of the detected groundwater contaminant. The task is to use computational modeling of the groundwater flow scenario in order to accurately identify the LUST. Of course, in real-world analyses, computational modeling such as this is just one prong of a multi-pronged analysis that includes sampling of the groundwater and conducting

geochemical tests that provide aging information and chemical degradation information, among other metrics.

The problem geometries that are considered in this work were selected for two reasons. First, they are fundamental and can be used as “building blocks” in the development of more sophisticated potential flow models. Second, each problem incorporates areas of extreme curvature in the flow regime, which are difficult to model computationally and require highly precise numerical models in order to obtain satisfactory results. Thus, the example problems are both challenging and relevant to problems of interest in the geosciences and other fields. For each problem, we develop two numerical approximations: (i) a coupled CVBEM/NPA model and (ii) an FEM model. The analytic solutions for these problems are known and given in [18]. The availability of the analytic solutions is important because it allows us to precisely quantify the computational error of the CVBEM and FEM models.

Each of the problems is formulated as a Dirichlet boundary value problem with boundary conditions specified from the target potential function. As a consequence of the Cauchy-Riemann equations, the CVBEM approximation of the target stream function can be developed directly based on the CVBEM approximation of the target potential function. That is, the CVBEM procedure allows us to generate streamlines using only boundary data from the potential function and vice-versa. However, for the FEM approach, the target streamlines must be developed using a post-processing vector gradient procedure.

Once the streamlines are developed, we identify the streamline going through the contamination site. Then, this streamline can be traced upstream to the source of the contamination. Thus, the LUST is determined as the candidate source point whose streamline goes through the contamination site. We assess accuracy by determining how well the streamlines generated by each numerical method trace the streamlines generated by the analytic solution. In particular, we are interested in whether each numerical method accurately identifies the LUST.

In the following problems, we assume the groundwater is represented by an ideal and incompressible fluid with no vorticity. Under these conditions, the velocity potential describing the groundwater flow situation is a scalar function satisfying Laplace’s equation. Thus, the problems are well-suited for modeling with the CVBEM.

3.1 Example Problem 1 - Potential Flow Around a Constrained Circular Obstruction

The analytic representation of the velocity potential for this problem is given in [18] as

$$\omega(z) = \pi \coth\left(\frac{\pi}{z}\right), \quad z \neq 0. \quad (5)$$

Since the exact solution is analytic everywhere except at $z = 0$, the real and imaginary parts of ω are harmonic functions in $\mathbb{C} \setminus \{0\}$. We employed symmetry of the flow situation to justify only modeling the right half of the modeling area of interest. This approach made it possible to remove the branch cuts associated with the analytic solutions from the problem domain, thereby making modeling using the CVBEM feasible.

Table 1: Example Problem 1 - Problem Description

Problem Domain:	$\Omega = \{(x, y) : 0 \leq x \leq 4, 0 \leq y \leq 6, \text{ and } x^2 + (y + 1)^2 \geq 1\}$
Governing PDE:	$\nabla^2 \psi = 0$
Boundary Conditions:	$\phi(x, y) = \Re[\pi \coth(\frac{\pi}{z})], \quad (x, y) \in \partial\Omega$
Number of Candidate Computational Nodes for CVBEM Model:	500
Number of Candidate Collocation Points for CVBEM Model:	1,000
Number of Nodes for FEM Model:	154,769
Number of Elements for FEM Model:	306,176

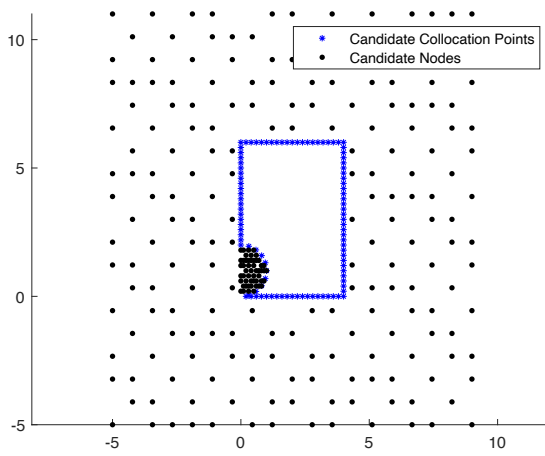


Figure 1: Problem setup for CVBEM model depicting candidate nodes and candidate collocation points. For visualization purposes, only 10% of the candidate collocation points and 50% of the candidate computational nodes are shown.

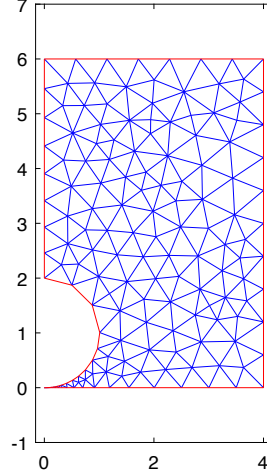


Figure 2: Problem setup for FEM model depicting the domain mesh. For visualization purposes, only 0.13% of the nodes and 0.09% of the elements are shown.

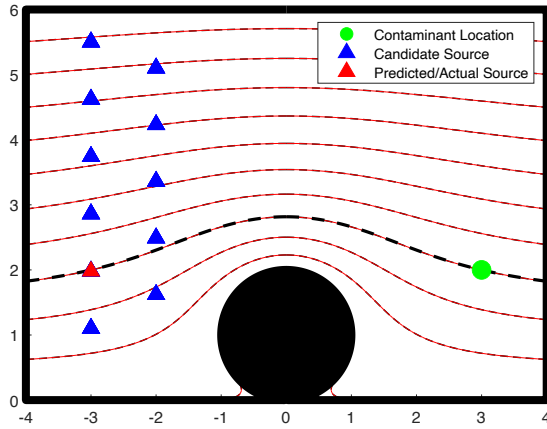


Figure 3: CVBEM computational outcome. In this case, the CVBEM model accurately tracks the target streamline (shown as a dashed black line) and correctly identifies the LUST. The streamlines were obtained from the potential outcomes as a consequence of the Cauchy-Riemann equations.

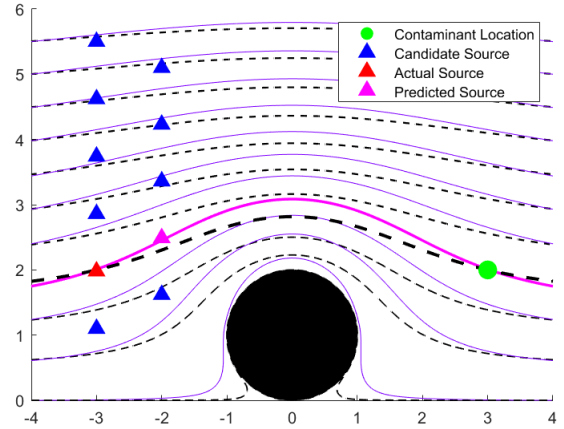


Figure 4: FEM computational outcome. In this case, the FEM model fails to accurately track the target streamline (shown as a dashed black line) and incorrectly identifies the LUST.

3.2 Example Problem 2 - Potential Flow Around a Free Circular Obstruction

We consider another potential flow problem with Dirichlet boundary conditions. This problem models potential flow around a free circular obstruction. The analytic representation of the velocity potential for this problem is given by:

$$\omega(z) = z + \frac{1}{z} + i \frac{3\pi}{4} \log(z), \quad z \neq 0. \quad (6)$$

The solution given in Equation (6) is analytic everywhere except at $z = 0$. Therefore, the real and imaginary parts of ω are harmonic functions in $\mathbb{C} \setminus \{0\}$. We employed symmetry of the flow situation to justify only modeling the right half of the modeling area of interest. Therefore, the computational outcomes depicted in the left half of the modeling area of interest were obtained by reflecting the outcomes in the right half. Constructing the problem domain in this way avoids the branch cut associated with the analytic solution, which makes it possible to model this problem using the CVBEM.

Table 2: Example Problem 2 - Problem Description

Problem Domain:	$\Omega = \{(x, y) : 0 \leq x \leq 6, -4 \leq y \leq 4, \text{ and } x^2 + y^2 \geq 1\}$
Governing PDE:	$\nabla^2 \phi = 0$
Boundary Conditions:	$\phi(x, y) = \Re \left[z + \frac{1}{z} + i \frac{3\pi}{4} \log(z) \right]$
Number of Candidate Computational Nodes for CVBEM Model:	500
Number of Candidate Collocation Points for CVBEM Model:	1,000
Number of Nodes for FEM Model:	7,833
Number of Elements for FEM Model:	153,360

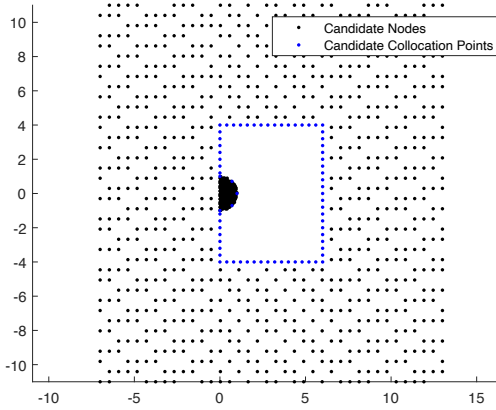


Figure 5: Problem setup for CVBEM model depicting candidate nodes and candidate collocation points. For visualization purposes, only 7% of the candidate collocation points are shown.

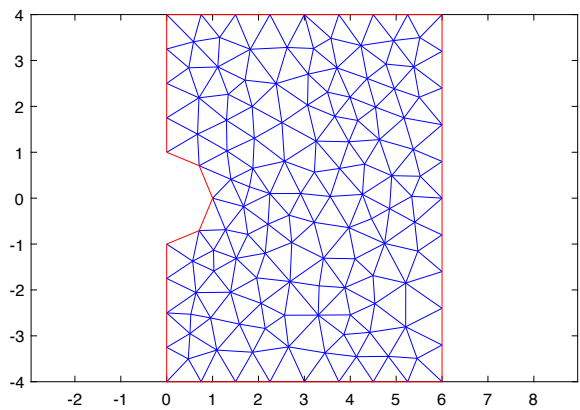


Figure 6: Problem setup for FEM model depicting the domain mesh. For visualization purposes, only 1.78% of the nodes and 1.56% of the elements are shown.

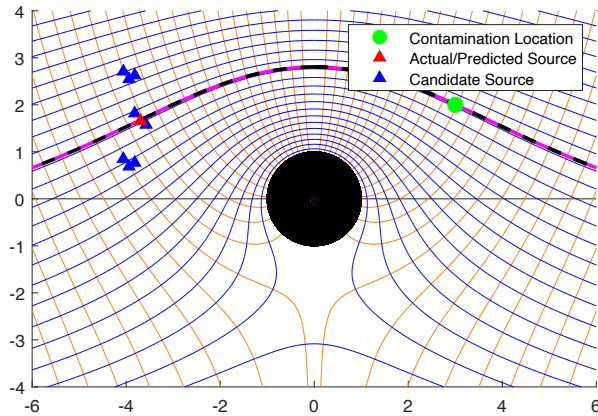


Figure 7: CVBEM computational outcome. In this case, the CVBEM model accurately tracks the target streamline (shown as a dashed black line) and correctly identifies the LUST. The streamlines were obtained from the potential outcomes as a consequence of the Cauchy-Riemann equations.

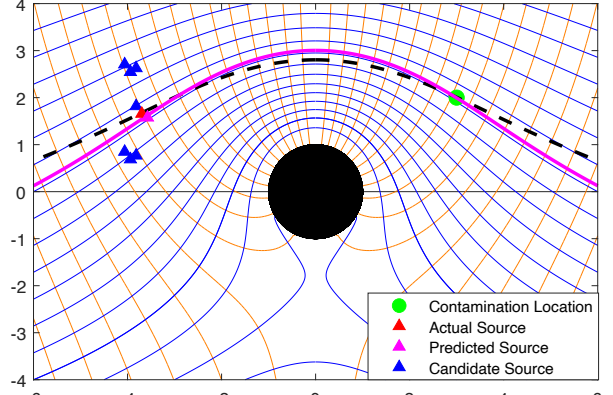


Figure 8: FEM computational outcome. In this case, the FEM model fails to accurately track the target streamline (shown as a dashed black line) and incorrectly identifies the LUST.

3.3 Example Problem 3 - Potential Flow Around a Wall Barrier or Foundation

We consider another potential flow problem with Dirichlet boundary conditions. This problem models potential flow around a wall barrier or foundation. The analytic representation of the velocity potential for this problem is given by:

$$\omega(z) = (z^2 + 4^2)^{1/2}, \quad z \neq 4i. \quad (7)$$

The solution given in Equation (7) is analytic everywhere except at $z = 4i$. Therefore, the real and imaginary parts of ω are harmonic functions in $\mathbb{C} \setminus \{4i\}$. We employed symmetry of the flow situation to justify only modeling the right half of the modeling area of interest. Therefore, the computational outcomes depicted in the left half of the modeling area of interest were obtained by reflecting the outcomes in the right half. Furthermore, we made an indentation on the left edge of the problem boundary in order to avoid the branch point at $4i$ of the analytic solution, thereby making modeling using the CVBEM feasible. The indentation makes the problem domain $\Omega = \Omega_1 \setminus \Omega_2$, where Ω_1 and Ω_2 are defined as follows:

$$\begin{aligned} \Omega_1 &= \{(x, y) : 0 \leq x \leq 4, 0 \leq y \leq 8\} \\ \Omega_2 &= \{(x, y) : 0 \leq x \leq 0.25, 0 \leq y \leq 4.25\}. \end{aligned} \quad (8)$$

Table 3: Example Problem 3 - Problem Description

Problem Domain:	$\Omega = \Omega_1 \setminus \Omega_2$
Governing PDE:	$\nabla^2 \phi = 0$
Boundary Conditions:	$\phi(x, y) = \Re \left[(z^2 + 4^2)^{1/2} \right]$
Number of Candidate Computational Nodes for CVBEM Model:	1,000
Number of Candidate Collocation Points for CVBEM Model:	2,000
Number of Nodes for FEM Model:	177,521
Number of Elements for FEM Model:	353,280

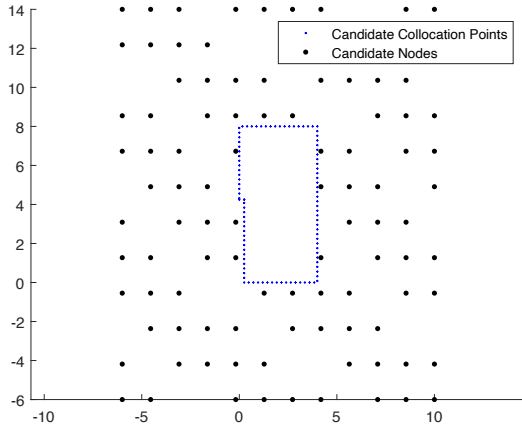


Figure 9: Problem setup for CVBEM model depicting candidate nodes and candidate collocation points. For visualization purposes, only 10% of the candidate collocation points and 10% of the candidate computational nodes are shown.

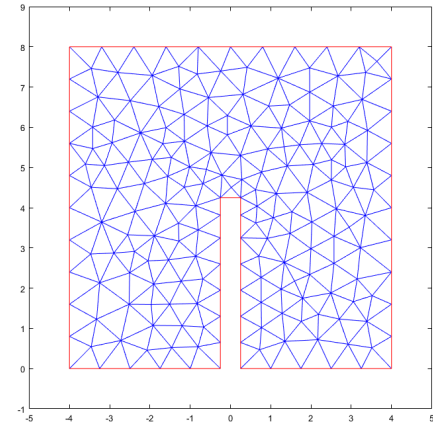


Figure 10: Problem setup for FEM model depicting the domain mesh. For visualization purposes, only 0.11% of the nodes and 0.09% of the elements are shown.

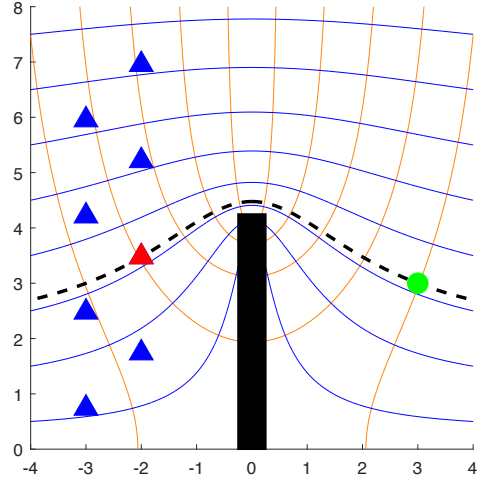


Figure 11: Depiction of the problem situation with the location of the accumulated contaminant shown as a green dot. The non-leaking candidate source points are shown as blue triangles, and the actual LUST is shown as a red triangle.

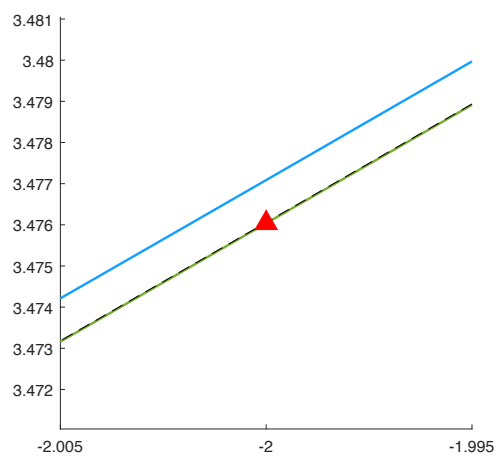


Figure 12: Zoomed-in comparison of the CVBEM and FEM numerical outcomes. In this case, the CVBEM streamline, shown in green, accurately tracks the target streamline, which is shown as a black dashed line. The FEM streamline, shown in blue, is north of the target streamline and does not accurately identify the LUST.

4 DISCUSSION AND CONCLUSION

The CVBEM has been used to model groundwater contaminant transport problems since at least as early as 1986 [19]. In this paper, we consider an important problem in groundwater transport; namely the identification of a LUST when contamination has been detected downstream from a set of several possible sources. These types of problems are often approached using geochemical analyses. However, the outcomes of such analyses can be buttressed by computational outcomes such as those that are shown in this work.

In this work we examined three Dirichlet BVPs of the Laplace type. The first example problem considers potential flow around a constrained circular obstruction. The second example problem considers potential flow around a free circular obstruction. And the third example problem considers potential flow around a wall barrier or foundation. These demonstration problems involve the computational difficulty of modeling flow regimes with regions of extreme curvature. The areas of extreme curvature require extra modeling attention and computational effort in order to obtain results with satisfactory accuracy, which makes these problems interesting and relevant to the geosciences and other fields. In the example problems, we employed the symmetry of the flow situations to justify only modeling the right half of the modeling area of interest. Therefore, the computational outcomes depicted in the left half of the modeling area of interest were obtained by reflecting the outcomes in the right half.

The CVBEM models used herein employ a recently-developed NPA from our research group, which has been shown to select highly efficient locations for computational nodes and collocation points such that the CVBEM model is capable of achieving an accurate solution while using relatively few terms in the approximation function [9]. These CVBEM models were compared with FEM models of the same problems that were developed using the PDE Modeler application within the program MATLAB. The CVBEM models correctly identified the LUST in the three problems that were examined, but the FEM models did not correctly identify the LUSTs. Part of the error of the FEM models came from the post-processing step of computing the gradient of the modeling outcome in order to obtain streamlines from the computed potential values. However, this step was not necessary in the CVBEM modeling as a consequence of the Cauchy-Riemann equations. The additional accuracy provided by CVBEM models for these problems can be of immense importance as the ability or inability to track groundwater contamination can trigger environmental, health, and legal repercussions.

ACKNOWLEDGEMENTS

The authors are grateful to Hromadka & Associates, a consulting firm, for supporting this research.

REFERENCES

- [1] Hromadka II, T. & Guymon, G., Application of a Boundary Integral Equation to Prediction of Freezing Fronts in Soil, *Cold Regions Science and Technology*, **6**, pp. 115–121, 1982.

- [2] Hromadka II, T.V. & Guymon, G.L., A Complex Variable Boundary Element Method: Development, *International Journal For Numerical Methods Engineering*, **20**, pp. 25–37, 1984.
- [3] Wilkins, B.D., Greenberg, J., Redmond, B., Baily, A., Flowerday, N., Kratch, A., Hromadka II, T.V., Boucher, R., McInvale, H.D. & Horton, S., An Unsteady Two-Dimensional Complex Variable Boundary Element Method, *SCIRP Applied Mathematics*, **8**(6), pp. 878–891, 2017.
- [4] Wilkins, B.D., Hromadka II, T.V. & Boucher, R., A Conceptual Numerical Model of the Wave Equation Using the Complex Variable Boundary Element Method, *Applied Mathematics*, **8**(5), p. 724, 2017.
- [5] Hromadka II, T.V., *A Multi-Dimensional Complex Variable Boundary Element Method*, volume 40 of *Topics in Engineering*, WIT Press, Southampton and Boston, 2002.
- [6] Hromadka II, T. & Whitley, R., Approximating three-dimensional steady-state potential flow problems using two-dimensional complex polynomials, *Engineering Analysis with Boundary Elements*, **29**, pp. 190 – 194, 2005.
- [7] Hromadka II, T. & Zillmer, D., Boundary element modeling with variable nodal and collocation point locations, *Advances in Engineering Software*, 2011.
- [8] Demoes, N.J., Bann, G.T., Wilkins, B.D., Grubaugh, K.E. & Hromadka II, T.V., Optimization Algorithm for Locating Computational Nodal Points in the Method of Fundamental Solutions to Improve Computational Accuracy in Geosciences Modeling, *The Professional Geologist*, 2019.
- [9] Wilkins, B.D., Hromadka II, T. & McInvale, J., Comparison of Two Algorithms for Locating Computational Nodes in the Complex Variable Boundary Element Method (CVBEM), *International Journal of Computational Methods and Experimental Measurements*, 2020 (in press).
- [10] Brebbia, C.A., *The Boundary Element Method for Engineers*, Wiley, 1978.
- [11] Brebbia, C. & Wrobel, L., Boundary element method for fluid flow, *Advances in Water Resources*, **2**, pp. 83–89, 1979.
- [12] Young, D., Chen, K., Chen, J. & Kao, J., A Modified Method of Fundamental Solutions with Source on the Boundary for Solving Laplace Equations with Circular and Arbitrary Domains, *Computer Modeling in Engineering and Sciences*, **19**(3), pp. 197–221, 2007.
- [13] Fornberg, B. & Flyer, N., Fast generation of 2-D node distributions for mesh-free PDE discretizations, *Computers and Mathematics with Applications*, **69**, pp. 531–544, 2015.
- [14] Hromadka II, T.V., Complex boundary elements for contaminant transport, *Environmental Software*, **6**(2), pp. 81–86, 1991.

- [15] Rasmussen, T.C. & Yu, G.Q., Complex Variable Boundary Integral Modeling of Groundwater Flow and Transport, in K.J. Hatcher, ed., *Proceedings of the 1997 Georgia Water Resources Conference*, The University of Georgia, 1997.
- [16] Rasmussen, T.C. & Yu, G.Q., A complex variable boundary-element strategy for determining groundwater flownets and travel times, *Advances in Water Resources*, **26**, pp. 395–406, 2003.
- [17] Brown, J.W. & Churchill, R.V., *Complex Variables and Applications*, McGraw-Hill, 8 edition, 2009.
- [18] Kirchhoff, R.H., *Potential Flows Computer Graphic Solutions*, CRC Press, 1985.
- [19] Hromadka II, T.V. & Yen, C.C., A model of groundwater contaminant transport using the CVBEM, *Computational Mechanics*, **1**(2), pp. 105–113, 1986.
- [20] Johnson, A.N. & Hromadka II, T.V., Modeling mixed boundary conditions in a Hilbert space with the complex variable boundary element method (CVBEM), *MethodsX*, **2**, pp. 292–305, 2015.